Computer-Aided Civil and Infrastructure Engineering **16(6)** (2001) 431–443

INDUSTRIAL APPLICATION

The Role of Computer Models in Full-Scale Bridge Laboratory Tests

D. G. Linzell *

Department of Civil and Environmental Engineering, The Pennsylvania State University, 231L Sackett Building, University Park, Pennsylvania 16801, USA

Abstract: *The role of computer modeling in an extensive series of curved steel bridge laboratory tests recently completed at the Federal Highway Administration's (FHWA) Turner-Fairbank Highway Research Center (TFHRC) is discussed. Computer models were involved extensively throughout the process, from design of the testing frame to analysis of data that were produced. Predicted results from a series of finite-element models are compared with data recorded from nine tests that occurred during construction. Results from the tests and from finite-element analyses are also compared against those produced using the V-load method, a simplified curved bridge analysis tool. The use of computer-generated Monte Carlo simulations to help reduce and analyze data generated during the construction tests is also discussed.*

1 INTRODUCTION

Computer modeling continues to play an important role in the experimental study of bridges and other structures. Comprehensive computer models help not only with designing the frame, fixtures, and components involved in the experiments but also with instrumentation placement, test planning, and data reduction and analysis. The importance of accurate computer modeling is magnified when bridge components or systems are tested at full scale.

Comprehensive computer modeling was an essential part of a series of full-scale curved steel bridge experimental investigations performed at the Federal Highway Administration's (FHWA) Turner-Fairbank Highway Research Center (TFHRC) in McLean, Virginia. The tests were used to investigate the behavior of curved steel plate girder bridges during construction and under loads causing predominantly flexural behavior. Results from the models provided confidence to the research team that desired behavior occurred and that pertinent data were collected and reduced.

A number of design iterations were performed before a final experimental bridge system was selected, fabricated, constructed, and tested. After the iterations were completed, a simply supported three-girder structure was selected (Figure 1).

A series of tests was performed as this structure was being constructed. They examined various subassemblies of the final three-girder system elastically under self-weight. Figure 2 indicates that a total of nine tests of six different framing plans were completed.

This article provides an overview of finite-element models that were constructed to help with the design and construction testing phases. Comparisons between data from the construction tests and finite-element predictions are presented and discussed. Additional examinations of analytical results from the finite-element models and from hand calculations using the V-load method are also shown. Finally, a series of computer-based Monte Carlo simulations, which were used to study the influences of instrument variability on data produced from the tests, are discussed.

2 PREVIOUS RESEARCH

A large number of computer and experimental studies of curved bridge behavior have been completed since the late 1960s. During this period, the advantages of constructing steel bridges using curved beams became more apparent, and a subsequent need for design specifications arose. Relevant publications from this time period will be summarized. Detailed discussions of curved steel bridge research are given by Zureick et al.,[30] Zureick and Naqib,[29] and Linzell.[19]

* E-mail: *dlinzell@engr.psu.edu.*

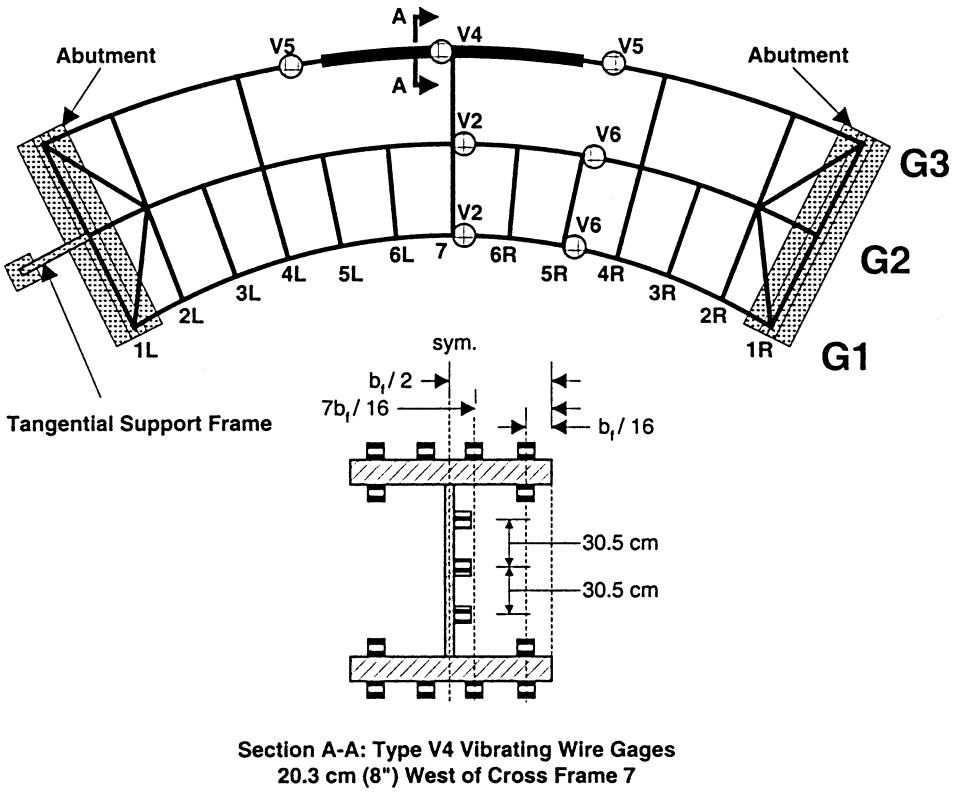

Fig. 1. Final experimental structure plan showing girder strain gauge instrumentation.

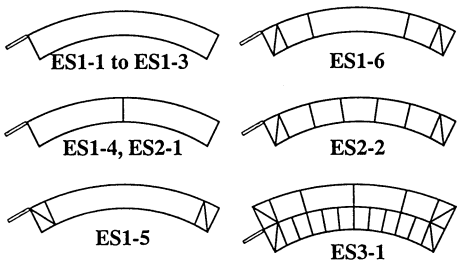

Fig. 2. Erection study framing plans.

To date, two specifications have been developed for the design of curved steel bridges: (1) the *AASHTO Guide Specifications for Horizontally Curved Bridges*[1] in the United States and (2) the *Hanshin Expressway Public Corporation's Guidelines for the Design of Horizontally Curved Girder Bridges*[15] in Japan. Organized development of the *AASHTO Guide Specifications* began with the Consortium of University Research Teams (CURT) Project in the late 1960s. The *Hanshin Guidelines* were compiled from Japanese research completed in the late 1970s and early 1980s. Both specifications incorporated a number of scale-model system tests and medium-scale component tests to investigate the behavior of curved steel bridges under static loads. Computer analyses were performed concurrently with many of these tests to help validate analytical results and to provide a mechanism for future studies of curved steel bridge behavior.

Culver and Christiano[9] performed static tests on a one-thirtieth scale model of a two-span continuous-curved I-girder bridge. Strains and deformations were compared with predictions from a computer program that used the flexibility method and influence coefficients derived directly from curved beam governing differential equations to obtain a solution.

Brennan[4,5] performed an extensive series of curved steel bridge analytical and experimental studies. Work centered on development of a three-dimensional (3D) computer program and on a series of experimental studies of a scale-model curved bridge. Comparisons between experimental and computer-generated influence lines, moments, and deflections for each curved girder were made. Further evaluation of the computer program was accomplished through comparisons with test results produced by Brennan et al.,[7] Brennan,[6] and Brennan and Mandel.[8]

Mozer et al.[21] examined the behavior of a pair of curved steel plate girders under high bending, high shear, and combined high bending and shear forces through eight static tests of a scale-model curved steel bridge. The structure was designed so that transverse stiffener and radial cross-frame locations could be varied. Results were compared with predictions from computer analyses that treated the system as a grid.

Fukumoto and Nishida[12] tested six simply supported curved I-beams and used data to validate a computer program for analyzing elastic and inelastic curved girder large deformation behavior. The beams had varying cross sections, span lengths, and radii of curvature and were tested under three-point bending. The program used transfer matrices along with the Runge-Kutta method to estimate deflections and ultimate strengths.

Yoo and Carbine[27] investigated the capacities of single rolled curved I-sections with differing cross sections and radii of curvature. Experimentally generated bifurcation loads from three-point tests were compared with computer-generated results.

Shanmugam et al.[24] and Thevendran et al.[25] compared finite-element results with experimental data from a series of isolated curved I-beam tests. Behavior of welded verses rolled curved beams was studied. The finite-element models were constructed using the ABAQUS finite-element analysis package and incorporated geometric nonlinearities and residual stress effects.

Static curved steel box-girder studies that involved testing and computer analyses included work by Fam and Turskstra,[10] which examined simply supported single-cell curved box girders under point and line loads. Experimental results were compared with data generated from finite-element analyses. Sennah and Kennedy[23] examined shear distributions in curved composite cellular box-girder bridges through extensive parametric studies using ABAQUS. Computer models were benchmarked against tests of four one-twelfth scale-model three-cell box-girder bridges. Composite box-girder behavior was examined by Arizumi et al.[3] using tests of a single simply supported specimen. Results were compared with predictions from a computer program using the finite-strip method.

While extensive effort has been dedicated to understanding the behavior of in-service curved steel bridges, little experimental or analytical research has been produced that focuses on their behavior during construction. Construction tests completed for the CSBRP attempted to address this research need. One extensive study of a curved I-girder bridge during construction was recently completed in the United States and reported on by Galambos et al.,[13] Pulver,[22] and Hajjar and Boyer.[14] Strains and deformations were recorded during construction (e.g., girder placement, concrete placement, etc.) of a two-span continuous horizontally curved and superelevated composite I-girder structure. Field results were compared with values produced from two curved bridge computer analysis programs and their accuracy assessed.

3 EXPERIMENTAL BRIDGE DESIGN

Design of the experimental bridge was strongly influenced by the primary goal of loading full-scale curved I-girder specimens to their full inelastic capacity while imposing realistic in situ boundary conditions.[28] Previously, many of the laboratory tests were conducted on either medium-scale isolated girders with unrealistic boundary conditions or on small-scale curved bridge systems where similitude could not be properly maintained for all relevant variables. Several configurations were investigated during the design phase of the experimental structure. The challenge associated with the design was to ensure linear elastic behavior of the portion of the structure outside any specimens that were tested (termed the testing frame) while inducing plastic deformations in each of the specimens. Initially, it was anticipated that a single full-scale girder could be used to examine flexural behavior. However, bracing of a single-girder system that would provide desired loads and boundary conditions to the specimens proved to be impractical. Twin-girder systems were investigated next. These systems also were abandoned because the interior girder would lift up and not remain elastic as load shifted from the exterior girder during plastification of the test specimen.

The structure selected for testing is shown in Figure 1. The three-girder system was designed so that under flexural loads the midspan portion G3 failed, while the remainder of the structure remained elastic, which permitted placement of plate girder specimens with differing geometric and material properties at this location. Girder spans along the arc were between 26.2 m for G1 and 28.6 m for G3 with radii of curvature between 58.3 and 63.6 m. Girder dimensions were between 121.9 × 0.8 cm and 121.9 × 1.3 cm for the webs and between 40.6 × 1.7 cm and 61.0 × 5.7 cm for the flanges.

Figure 1 indicates that extra lines of cross-frames were placed between G1 and G2 in the final structure. These cross-frames were used to stiffen and stabilize these two girders and to provide a load-distribution path that placed the highest forces at midspan of G3. To achieve this load-distribution path, cross-frames were constructed using five 413-MPa tubular steel members arranged in a K, as shown in Figure 3.

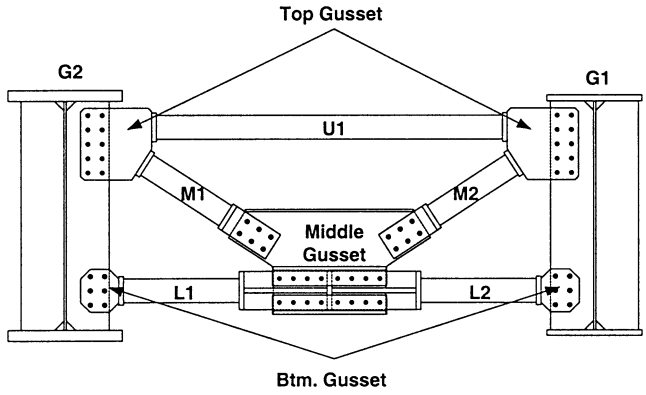

Fig. 3. Typical cross-frame elevation.

Girders were supported with radially oriented abutments consisting of steel W-sections and channels tied to the strong floor with DYWIDAG bars. These abutments elevated the system to a height of approximately 2 m off the laboratory floor. A combination of spherical bearings and Teflon pads were used to minimize frictional forces and allow translation and rotation in any direction except downward at the abutments for G1 and G3. G2's movement was restrained using guided bearings at both ends and a tangential support frame at its west end, as shown in Figure 1. The guided bearings prevented radial translation, and the tangential frame, consisting of W-sections and pinned to G2 at its neutral axis, helped stabilize the system. Differential radial displacement between adjacent girders was minimized through the use of lower lateral bracing mounted diagonally between adjacent girders in the exterior cross-frame bays.

The preliminary finite-element analyses of this structure indicated that once the specimens at midspan of G3 began to yield, the load shifted from G3 to G2. To resist this load increase elastically, the ASTM A572 grade 50 steel originally planned for G2 was replaced with AASHTO M270 grade 70W. G1 and G3 were constructed of grade 50 steel.

Illustrated in Figure 4 is a plan view of the finite-element model that was assembled to predict behavior of the experimental bridge for preliminary analyses of the construction tests. The model was developed using the PATRAN Version 3.0[20] solid modeling package and was converted to ABAQUS/Aqua Version 5.5[16–18] for analysis. ABAQUS was selected for the experimental bridge models because of its advanced geometric and material nonlinear modeling capabilities and its extensive element libraries. The model that is shown was for the final construction test, ES3-1, and had over 8400 elements and over 50000 degrees of freedom. Additional lines superimposed onto each cross-frame in Figure 4 represent ABAQUS mass elements placed at cross-frame connection points to simulate the self-weight of these connections.

Finite-element models used to predict construction test response were similar to those used to provide preliminary predictions of test specimen behavior.[28] They were constructed so that an accurate measure of each specimen's behavior in the linear and nonlinear ranges was obtained. Considerations also were given to the computer system used for the analyses and to obtaining an accurate prediction of the elastic response of the "testing frame" during each specimen test so that premature and unforeseen yielding could be avoided. These three criteria helped dictate the density, type, and distribution of the elements. G3, which contained the test specimens, was the girder that received the highest level of detail in the models. G1 and G2 had lower levels of discretization and contained less-sophisticated elements. Other items of importance that were considered during development of the models were accurate and efficient measurement of loads in cross-frame and bracing members, correct replication of girder support conditions, and effective reproduction of the dead-load distribution.

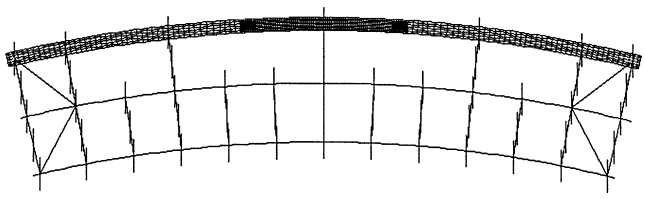

Fig. 4. Plan view of ABAQUS finite-element model for ES3-1.

3.1 Discretization

Finite-element models of the construction tests subdivided the bridge into three groups: the three support girders outside the construction/flexural specimens (the *testing frame*), the specimens themselves, and the cross-frames and lower lateral bracing. Node placement and resulting element distributions differed depending on which group was being addressed. Abutments and the tangential frame used to restrain the system (see Figure 1) were not modeled explicitly and were incorporated in the analyses as boundary conditions.

The testing-frame mesh used 5 shell elements through the web depth for G1 and G2 and 10 shell elements through the web depth for G3. G1 and G2 flanges were modeled using beam elements, whereas G3 flanges used 6 shell elements across their width. Ten elements typically were placed between cross-frame connection locations along the length of all three girders. At certain points along the girders, nodal lines were switched from this pattern to accommodate additional stiffeners required at support and loading points. Nodal patterns in the test specimens were increased from those in the testing frame so that 14 elements existed through the web depth and 10 elements across the flanges. Solid triangular and rectangular elements were used to simulate the splice plates between the testing frame and the specimens. Cross-frames and the lower lateral bracing were modeled as beam elements with nodes located at the ends and at midlengths of these members. ABAQUS elements used for the structural components are summarized in Table 1. "ES" represents the section spliced at midspan of G3 for the construction tests.

3.2 Boundary conditions

Spherical bearings were provided at the abutments for G1 and G3 to allow rotation about any axes and translation in any direction except downward. Corresponding nodes at the abutments had their vertical translational degrees of freedom restrained, with all other degrees of freedom unrestrained. G2 had similar constraints at its ends, but

Table 1
ABAQUS element summary

Location	*Structural component*	*ABAQUS element type*
G1, G2, G3, ES	Web	S4R
G1, G2	Flanges	B31
G3, ES	Flanges	S4R
G1, G2	Stiffeners	B31
G3, ES	Stiffeners	S4R
G1–G2, G2–G3	Cross-frame members	PIPE32
G1–G2, G2–G3	Lower lateral bracing	B32
G3, ES	Splice plates	C3D6, C3D8

radial translation also was prevented using guided bearings. ABAQUS GAPUNI unidirectional gap elements, with lengths equal to bearing shim pack heights, were implemented at each girder abutment support to account for frictional forces that could be induced into the system should a Teflon pad unexpectedly stick. The support frame at the west end of G2 was connected to the girder web using a pin placed within a vertically aligned slotted hole. This theoretically prevented any movement in the tangential direction while allowing the remaining translations and rotations to occur. The analytical model mimicked this restraint. Intermediate shoring points used during the construction tests were accounted for by restraining corresponding nodes at the bottom flanges of G1, G2, and G3.

3.3 Geometric and materials properties

Geometric information for the analyses differed depending on the type of ABAQUS element used to represent each structural component. Finite-element simulations of the construction tests were performed initially using nominal dimensions from the design plans. The models were then reanalyzed with actual dimensions calculated as averages of measurements taken during construction. In general, measured dimensions were slightly larger than nominal dimensions.

Materials properties used in the ABAQUS model were taken initially from nominal values specified in the design plans. Modifications to these values were made based on results from manufacturer certification reports and from coupon tests that were performed.

3.4 Loading conditions

Loads for the construction test finite-element models consisted of self-weights of the bridge components. To account for member weights, steel densities were entered and were set equal to the standard value for rolled steel, namely, 77 kN/m^3. Additional mass elements were required at each cross-frame member connection due to the large number of gusset plates used at these connections (see Figure 3).

4 TESTING

4.1 Instrumentation

Construction tests were divided into three groups: ES1 series tests, ES2 series tests, and ES3 series tests. They examined the behavior of the framing plans in Figure 2 as shoring was sequentially removed and replaced. ES1 series tests involved shoring removal and replacement from beneath G1, ES2 tests from beneath G1 and G2, and ES3-1 from beneath all three girders.

Data were recorded during shoring removal and replacement. A large number of instruments was required to provide accurate measure of behavior during both the construction tests and the flexural tests that followed. Finite-element analyses were an important part of instrument selection and placement. Types, locations, and densities of instruments were determined using results from computer analyses performed during the design phase.

Instruments for the construction and flexural tests consisted of

- Load cells and instrumented studs to measure support reactions and applied loads
- Vibrating wire and resistance strain gauges to measure strains developed during construction and testing
- Displacement and rotation transducers (LVDTs, potentiometers, and tiltmeters) to measure deformations developed at select cross sections during construction and testing
- Targets for laser and total station systems to measure global deformations experienced during construction and testing

A large percentage of this instrumentation was affixed to G3 and the cross-frames between G2 and G3. G3 contained specimens examined during the flexural tests, and therefore, a number of data points were required near midspan to track each specimen's elastic and inelastic behavior. Cross-frame members between G2 and G3 were instrumented to ensure that they remained elastic and to provide internal force measurements for any necessary free-body diagrams.

Instruments required for the flexural tests were placed onto the structure during construction and helped record data during the construction tests. Load cells were positioned at girder support points and at abutments and intermediate shoring locations. Strain gauges were affixed to the girders, cross-frames, and lower lateral bracing. Figure 1 details locations for girder strain-gauged sections for the construction tests and shows gauge positions at midspan of G3. Deformation transducers were placed at midspan and at the supports of each girder. Laser and total station systems were used to track global deformations and acquired targets on the girder top and bottom flanges.

Since instruments required for the flexural tests were used for the construction tests, the quantity of instrumenta-

tion available for acquisition increased as components were added to the structure. Over 1050 data points were recorded during each testing step for ES3-1.

4.2 Testing procedure

The construction tests were performed to

- Provide insight into curved steel bridge behavior during construction
- Establish confidence in the finite-element models
- Help coordinate methods for identifying and storing data generated during testing

The tests followed a standard procedure. Each began with the system shored to its "no load" position. This position theoretically represented a shored condition in which all dead-load strains and deformations had been removed. It was established for each test using a combination of field-measured girder camber information and results from preliminary analyses. Information from the analyses and the camber data was used to obtain reasonable "no load" positions in the laboratory using abutment and shoring load cells and midspan potentiometers. A large number of iterations typically were required to establish an acceptable "no load" position.

Once an acceptable "no load" position was established for each test, a series of shoring removal steps was used to lower the girder(s). Once the girder(s) were lowered, shoring was sequentially replaced to return the system to its initial "no load" position. The first three tests, ES1-1 to ES1-3, involved G1 and G2 with cross-frames 1L and 1R in place (see Figure 2). Shoring was removed and replaced sequentially from beneath G1 for each of the tests while G2 remained shored. ES1-4 and ES2-1 studied G1 and G2 with cross-frames 1L, 7, and 1R in place. ES1-4 examined this system as shoring was removed and replaced sequentially from beneath G1. ES2-1 studied the system as shoring was removed sequentially from beneath G1, followed by sequential shoring removal from beneath G2. Once the maximum predicted elastic deformation had been reached, shoring was replaced beneath both girders. ES1-5 examined a framing plan that involved cross-frames 1L, 1R, 2L, and 2R as shoring was removed from beneath G1. ES1-6 involved cross-frames 1L, 1R, 2L, 2R, 4L, and 4R. ES2-2 was the second test that studied behavior as shoring was removed and replaced from beneath both G1 and G2. The system that was tested involved the lower lateral bracing and cross-frames 1L, 2L, 4L, 6L, 4R, 2R, and 1R. ES3-1 was the single test in which shoring supports were removed and replaced sequentially from beneath three girders. Thirteen cross-frames were in place between G1 and G2 and seven between G2 and G3. The system began in its "no load" position, and shoring was removed sequentially from beneath all three girders. A series of investigations of each girder using a single midspan shore was performed after the system had been lowered. G3 was raised and lowered in equal load increments followed by similar examinations of G2 and G1. At the completion of these single-girder investigations, the three-girder system was returned to its "no load" position.

5 EXPERIMENTAL AND ANALYTICAL COMPARISONS

5.1 Construction test data and finite-element analyses

Accuracy of finite-element models in the elastic range was assessed through detailed comparisons with experimental results for five of the construction tests: ES1-4, ES1-6, ES2-1, ES2-2, and ES3-1. The single (ES1-4, ES1-6) and twin-girder (ES2-1, ES2-2) tests were selected because they were judged to best represent actual twin-girder configurations that could be constructed in the field. The three-girder test was selected because it was similar to the framing plan used to perform the flexural tests. The shoring removal sequence followed during the tests was replicated in the finite-element models by removing corresponding nodal restraints.

Analytical and experimental support reactions, vertical displacements, and girder and cross-frame internal strains and forces were compared at various points during the tests. Although all the construction tests were elastic, comparisons that were performed provided a level of confidence in the finite-element models that was previously unavailable. In addition, they helped assess the need for the replacement, relocation, or addition of instrumentation prior to initiation of the flexural tests.

The first test that was examined experimentally and analytically was ES1-4. A support reaction versus midspan displacement plot for G1 is shown in Figure 5. The figure shows the variation in reactions at cross-frames 1L, 1R, and 7 as G1 was lowered. The shoring support at cross-frame 7 was used to lower G1 to its final deformed shape. Differences between experimental and analytical support reactions approached 6.5 kN, and displacements differed by 0.13 cm.

Explanations for discrepancies observed in Figure 5 are as follows. Zero shifts of experimental readings, which resulted from heating of the instruments and data acquisition system circuitry, occurred during establishment of the initial "no load" position. These shifts occurred for all the construction tests. In addition to the zero shifts, changes to the experimental structure, which could not be quantified, occurred during fabrication. When the girders were fabricated, G2 was incorrectly cambered and was heated and recurved to the correct camber. The heating and recambering made transverse stiffeners out of plumb and caused fit-up problems for the cross-frames, which, in turn,

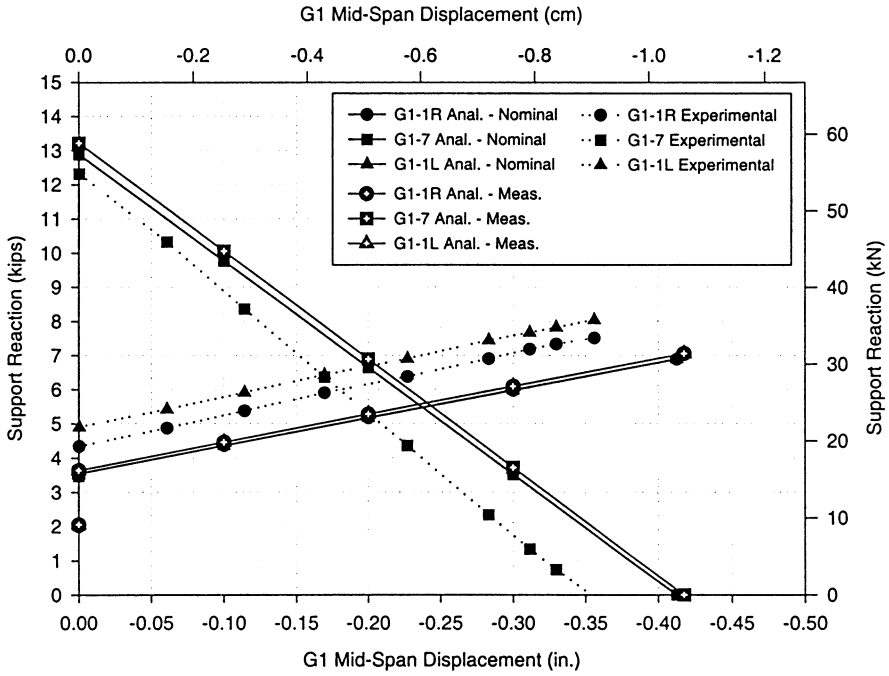

Fig. 5. Support reactions versus G1 midspan vertical displacement, ES1-4.

locked forces into the system that could not be accurately measured and incorporated into the finite-element model. Figure 5 shows that replacing nominal properties with measured values had little effect on the accuracy of analytical results.

Comparisons between experimental and analytical strains in the top and bottom flanges of G1 and G2 are shown in Figures 6 and 7. Experimental strains were obtained from vibrating wire gauges affixed to the exterior flange faces, whereas analytical values were from nodes at similar points in the model. Each figure examines the strain variations across the flange width when G1 had displaced 1.0 cm vertically. Lateral bending (bimoment) effects are clearly visible.

As had occurred for the support reactions, discrepancies between experimental and analytical top-flange strains did exist. These discrepancies were largely attributed to locked-in forces in the experimental structure that occurred during its construction. Replacing nominal geometric and material properties with measured properties again offered little improvement in analytical predictions.

Comparisons between experimental and analytical axial loads in the lower chord members in cross-frame 7 between G1 and G2 are shown in Figure 8. Refer to Figure 3 for the location of individual members in a typical cross-frame. Similar discrepancies and trends to previous comparisons are shown.

Representative comparisons for the final construction test, ES3-1, are plotted in Figures 9 to 11. The comparisons are made for G3 support reactions and strains and for axial forces in cross-frame 7 between G2 and G3. Note that since ES3-1 incorporated additional investigations using a single midspan shore, certain figures contain results from the first two shoring removal steps only.

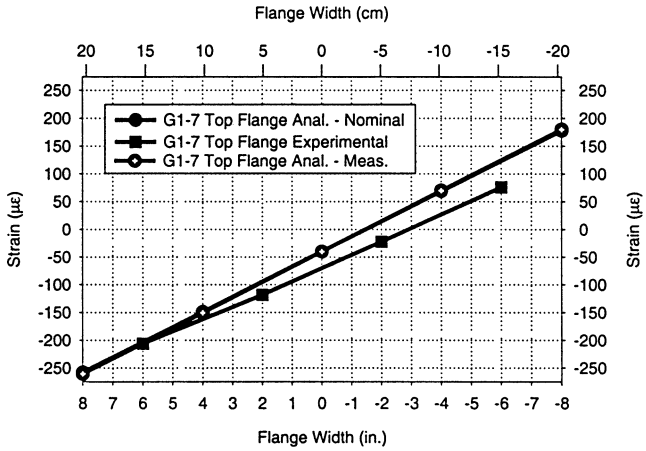

Fig. 6. G1 top flange strains at cross-frame 7, displacement = 1.0 cm, ES1-4.

Similar results to those discussed for ES1-4 are evident for the analytical and experimental comparisons made for ES3-1. Discrepancies between experimental and analytical values are evident and are attributed to zero shifts of the data and to locked-in forces being developed in the structure as it was being constructed. Cross-frames added to

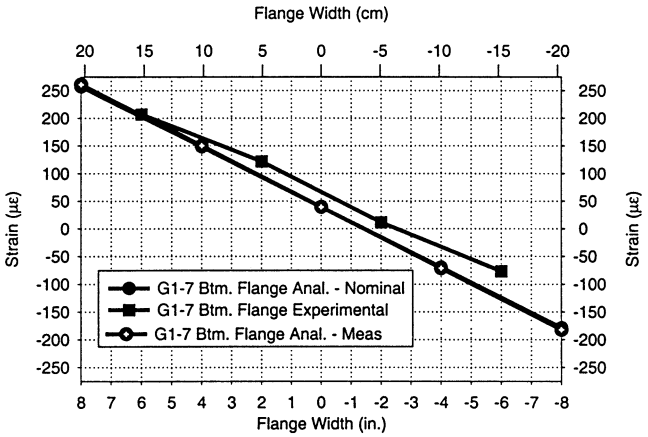

Fig. 7. G1 bottom flange strains at cross-frame 7, displacement = 1.0 cm, ES1-4.

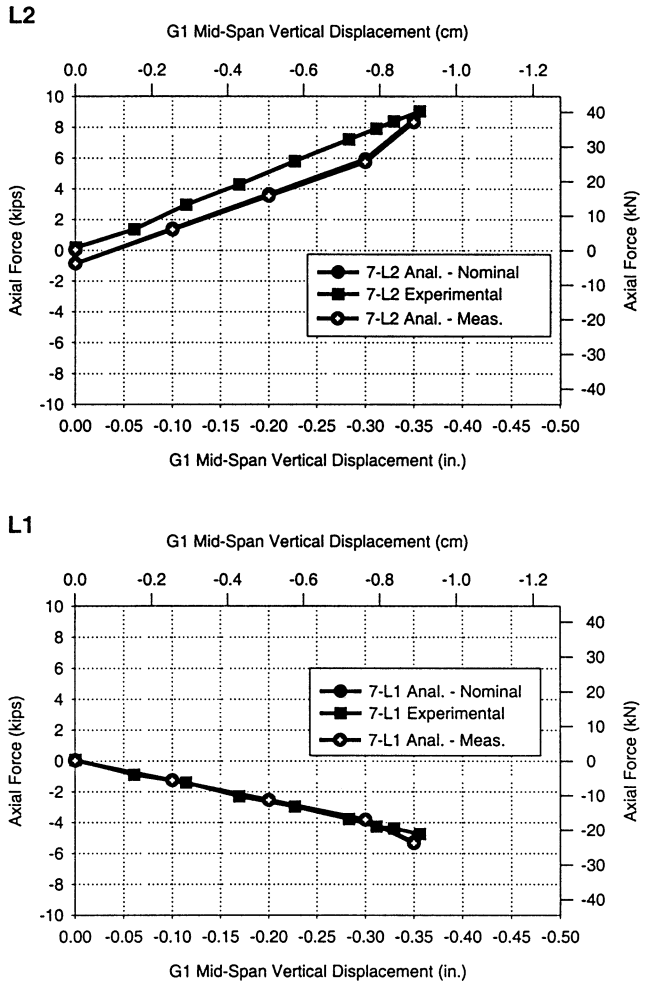

Fig. 8. Lower chord member axial forces versus G1 displacement, cross-frame 7 between G1 and G2, ES1-4.

the system to obtain the final ES3-1 configuration caused further redistribution of loads and subsequent increases in differences between experimental results and analytical predictions. While the levels of error in some of the plots may appear alarming, magnitudes typically were small when the size of the structure, its level of indeterminacy, and anticipated loads and deformations generated during the flexural tests were considered. As an example, a 31-kN difference between analytical and experimental support reactions was observed in Figure 9. This difference appears large but is approximately 5 percent of the total self-weight of the system, which was 521 kN.

5.2 Construction test data, finite-element and V-load analyses

It was of interest to compare results from the construction tests against those found using both ABAQUS analysis results and results from an approximate analysis method. The V-load method, as outlined by AISC,[2] was the approach chosen because it is one of the most common preliminary design tools used for curved steel bridges.

The V-load method was studied through comparisons of G1 and G3 midspan moments for ES3-1. Comparisons were made for the testing step in which the three-girder system had all intermediate shoring removed and was fully displaced under its own self-weight. Since the V-load method was derived for curved girder systems in which all cross-frame lines were continuous, it was decided that V-loads would be calculated assuming that cross-frames that existed only between G1 and G2 had been removed. ABAQUS analyses of the modified framing plan loaded under self-weight indicated that minimal changes to girder midspan moments occurred when the cross-frames were removed. Primary moments would be determined using measured dead loads, which included all cross-frames.

Midspan moments found using the V-load method and the finite-element model are compared with experimental moments for G1 and G3 in Table 2. Girder dead loads are found using as-built measurements. The table shows that both analytical and V-load results gave good estimates of experimental midspan moments for G3, with differences being 10 percent or less. V-load estimations for G1 midspan moment were not as accurate and were nonconservative, with a moment of −50 kN·m being predicted at midspan of G1, whereas the experimental magnitude was 41 kN·m. The ABAQUS model predicted the experimental midspan moment for G1 quite well. Even though the midspan moment magnitudes for G1 were small, the fact that the V-load method estimated negative bending at midspan of G1 showed that interior girder moment predictions using this approach could not be considered as accurate as those for the exterior girder. Studies by Fiechtl et al.[11] showed similar results to what was observed for

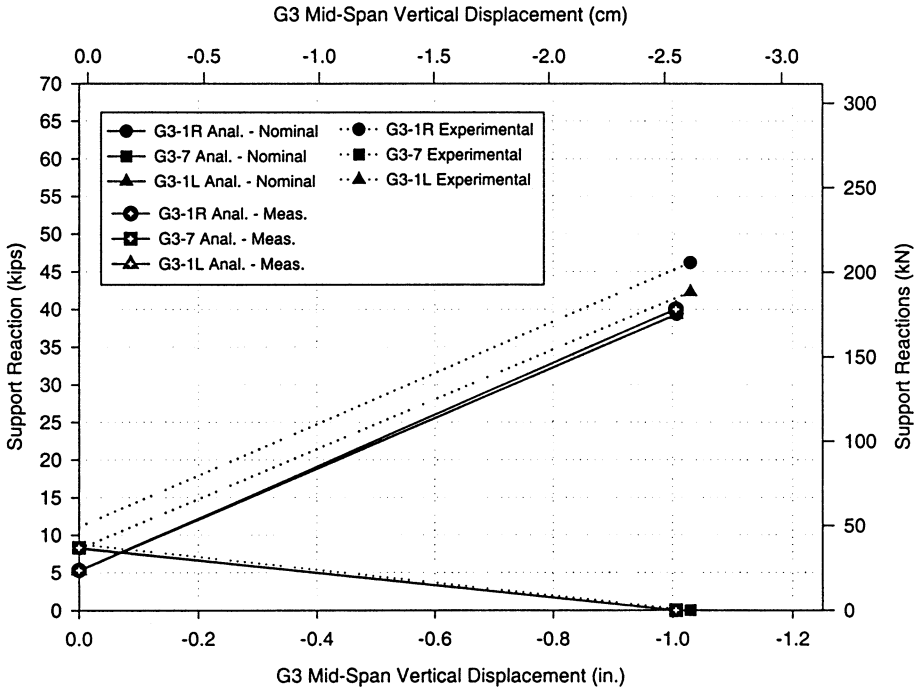

Fig. 9. Support reactions versus G3 midspan vertical displacement, ES3-1.

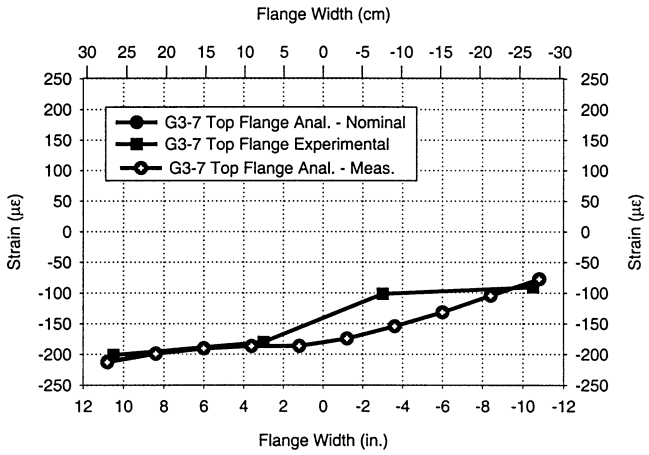

Fig. 10. G3 top flange strains at cross-frame 7, displacement = 2.5 cm, ES3-1.

here: V-load estimations of dead-load flexural behavior in the exterior girder were shown to be accurate, but nonconservative results could be obtained for the interior girder in a multigirder system.

6 MONTE CARLO SIMULATIONS

In addition to helping examine the accuracy of finite-element models used to analyze and design the structure, the construction tests provided a means for development and coordination of data reduction and storage methods for the flexural tests, which followed ES3-1 and involved higher loads and more sensors. One important part of the data reduction process was being able to resolve equilibrium of various free-body diagrams of the bridge. Being able to evaluate the equilibrium of portions of the structure with an acceptable level of accuracy not only was valuable for studying the validity of the data, but it also was important for determining the behavior of a portion of the structure (such as the midspan of G3) when loads and deformations exceeded an instrument's operating range. It was known prior to calculating equilibrium that certain items associated with the highly indeterminate structures that were tested, such as construction-sequence effects and material and geometric imperfections introduced during fabrication, would affect experimental results so that equilibrium in a theoretical sense (all force and moment components summing to zero) could not be achieved experimentally.

Table 2
G1, G3 midspan moments

	Midspan moment (kN· m)			*Difference from exp. (%)*	
Girder	*Exp.*	*FEM*	*V-Load*	*FEM*	*V-Load*
G1	41	39	−50	−3	−220
G3	1306	1395	1333	7	2

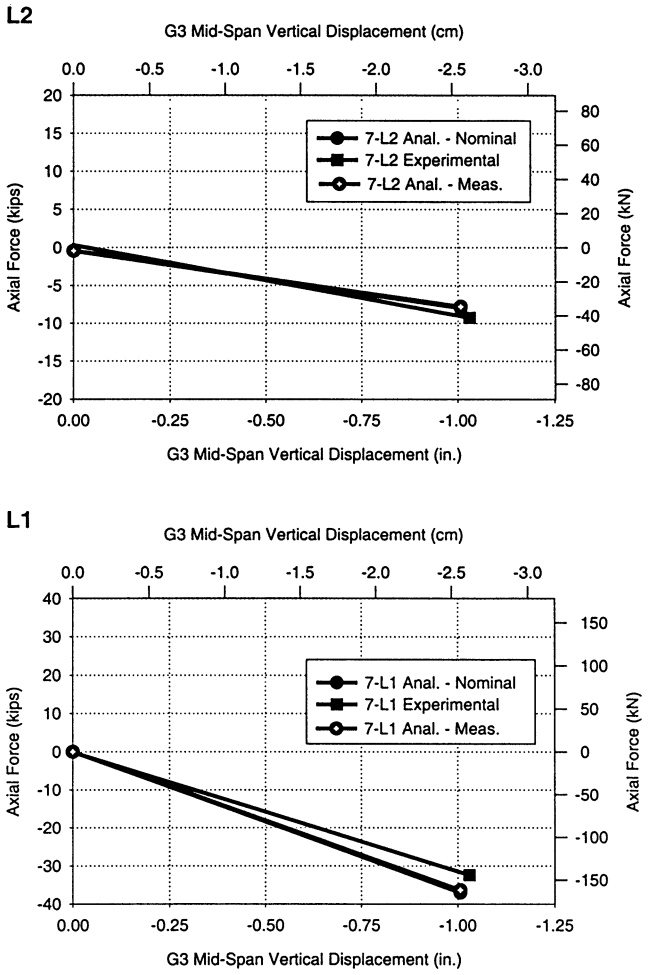

Fig. 11. Lower chord member axial forces versus G3 displacement, cross-frame 7 between G2 and G3, ES3-1.

Extensive effort was dedicated to developing and examining data reduction methods for calculating equilibrium of numerous free-body diagrams of the construction tests. The sensitivity of results generated from these equilibrium studies was examined using a series of computer-aided Monte Carlo simulations. The studies examined the effects of cumulative changes in instrument resolution on equilibrium results, which could result from electrical noise disturbing instrument signals and from using different data-acquisition systems, with varying levels of accuracy, to acquire the data. A commercially available software package, DecisionPro,[26] was selected to perform the Monte Carlo simulations. DecisionPro uses a decision tree to create the probabilistic model and all subsequent single-valued and random variables in that model.

The first step for the simulation was identification of the probabilistic model to be analyzed. Data from test ES1-3 were used to complete the simulation. The free-body diagram that was selected was the entire span of G1, which exposed internal forces in the two end cross-frames (1L and 1R) and was judged to be representative of all remaining equilibrium checks performed for the construction tests.

The six equations typically examined for equilibrium (force and moment sums about the three global coordinate axes) were reduced to two generic force and moment equations for simulation in DecisionPro. The numbers of force, unit, and distance vectors involved in the simulations were directly related to the number of active instruments for ES1-3 and their locations on the structure. All variables in the equations were either random in their own right or involved terms that were random.

Monte Carlo simulations were run for a single data set from ES1-3: the testing step in which the largest vertical displacements and rotations were generated at midspan of G1. Load and strain magnitudes from this data set were used to obtain initial means and standard deviations for the normal distributions that represented corresponding random variables in DecisionPro. Means and standard deviations for strain gauges affixed to cross-frames 1L and 1R are listed in Table 3. Data for the geometric variables required for calculating force and moment equilibrium were obtained from geometry measurements taken during construction. Normal distributions were used to represent these variables.

Standard deviations for certain random variables were increased from their initial settings, and effects on force and moment equilibrium obtained were examined. The first simulations calculated equilibrium using recorded data means and standard deviations from the cross-frame strain gauges. Strain gauge standard deviations were then increased to $5\mu\varepsilon$ to investigate sensitivity of calculated equilibrium to increased variability in gauge data. A standard deviation of $5\mu\varepsilon$ was approximately four times the values listed in Table 3, which appears to be a dramatic increase. However, 12-bit data acquisition systems were used to acquire the strain gauge data, and their readable ranges were set at $\pm$ 20,000$\mu\varepsilon$ so that resolutions greater than those shown in Table 3, between $10\mu\varepsilon$ and $20\mu\varepsilon$, were likely. Therefore, a third set of simulations with standard deviations of $10\mu\varepsilon$ and a final set with deviations of $20\mu\varepsilon$ also were examined. Results from the moment simulations are tabulated in Table 4.

The table indicates a general trend for the influences of strain gauge variability on moment equilibrium sums. It shows that while adjustments in the variability of strain gauge readings did not appreciably affect mean sum values (i.e., errors in the equilibrium calculations), they had greater influence on the standard deviations. When slight cumulative increases in the variability of the strain gauge readings was introduced, standard deviations for the corresponding moment equilibrium sums increased by upward of a factor of 10 from initial values. This indicates that equilibrium was sensitive to slight variations in strain gauge

Table 3
Cross-frame strain gauge means and standard deviations, ES1-3

Gauge ID	*Mean($\mu\varepsilon$)*	*Standard deviation ($\mu\varepsilon$)*	*Gauge ID*	*Mean ($\mu\varepsilon$)*	*Standard deviation($\mu\varepsilon$)*
S-1L-U1-T	−14.15	1.28	S-1R-U1-T	−41.45	0.90
S-1L-U1-E	−223.24	1.49	S-1R-U1-E	199.82	0.52
S-1L-U1-B	28.64	0.83	S-1R-U1-B	−20.05	0.76
S-1L-U1-W	214.65	1.04	S-1R-U1-W	−226.10	0.52
S-1L-M2-T	−47.51	0.90	S-1R-M2-T	−38.08	0.52
S-1L-M2-E	−707.96	1.04	S-1R-M2-E	659.78	0.83
S-1L-M2-B	−1.18	0.76	S-1R-M2-B	0.17	0.41
S-1L-M2-W	561.55	1.53	S-1R-M2-W	−705.94	0.83
S-1L-L2-T	24.94	0.83	S-1R-L2-T	−3.37	1.22
S-1L-L2-E	180.44	0.55	S-1R-L2-E	−21.90	0.83
S-1L-L2-B	82.22	1.22	S-1R-L2-B	91.65	0.52
S-1L-L2-W	−64.36	1.04	S-1R-L2-W	181.96	0.90

Table 4
Moment equilibrium means and standard deviations, G1 equilibrium, ES1-3

Component	*MC simulation*	*Equilibrium summation mean ($kN \cdot m$)*	*Equilibrium summation standard deviation ($kN \cdot m$)*
M_x	Raw data	91.3	6.4
	Strain gauge std. dev. = 5 $\mu\varepsilon$	91.1	18.3
	Strain gauge std. dev. = 10 $\mu\varepsilon$	90.8	36.6
	Strain gauge std. dev. = 20 $\mu\varepsilon$	90.1	73.3
M_y	Raw data	44.1	19.7
	Strain gauge std. dev. = 5 $\mu\varepsilon$	43.1	53.5
	Strain gauge std. dev. = 10 $\mu\varepsilon$	41.6	106.9
	Strain gauge std. dev. = 20 $\mu\varepsilon$	38.5	213.9
M_z	Raw data	−28.7	1.0
	Strain gauge std. dev. = 5 $\mu\varepsilon$	−28.7	2.6
	Strain gauge std. dev. = 10 $\mu\varepsilon$	−28.7	5.2
	Strain gauge std. dev. = 20 $\mu\varepsilon$	−28.6	10.4

readings. The moment components that exhibited the largest increases in standard deviations, moments about the x and y axes, were those which were influenced the most by cross-frame member forces (due to the member orientations) and by the moment arm through which those forces acted.

7 CONCLUSIONS

The role of computers during design and preliminary testing phases of the Curved Steel Bridge Research Project (CSBRP) is summarized. The CSBRP was instituted to study the behavior of full-scale curved steel bridge I-girders in a testing system that produced realistic load and boundary conditions.

Finite-element analysis was an important part of the experimental bridge system's iterative design process. A number of preliminary finite-element models were assembled in ABAQUS and were used to examine prototype testing systems to determine if desired behavior was achieved. These analyses helped determine that a simply supported three-girder system would provide the best simulation of actual full-scale curved I-girder behavior in the prescribed restraints of the laboratory used for testing. It also would provide a level of redundancy and safety that similarly sized single- and twin-girder systems could not.[28]

The first evaluations of the accuracy of finite-element models used during the design phase occurred when a series of tests of the selected experimental structure, a simply supported three-girder system, was performed while it was being constructed. The tests involved various subassemblies of the final structure and examined the behavior of each system elastically as intermediate shoring was removed and replaced. Comparisons between analytical predictions from ABAQUS and laboratory data occurred for

five of the tests: ES1-4, ES1-6, ES2-1, ES2-2, and ES3-1. Support reactions and midspan displacements, girder flange and web strains, and axial forces developed in individual cross-frame members were examined. These studies indicated that

- The detailed finite-element models gave good predictions of elastic behavior, given the size of the systems that were tested and their high levels of redundancy.
- Zero shifts, caused by heating of instruments and circuitry prior to testing, and locked-in forces introduced during construction that could not be quantified were the predominant causes of errors observed between the computer predictions and data.
- Replacing nominal geometric and material properties with measured properties offered little improvement in analytical predictions.

Additional comparisons between experimental and analytical results were made when girder midspan moments and cross-frame member axial forces produced during test ES3-1 were compared with analytical predictions from ABAQUS models and from the V-load method. These comparisons indicated that the V-load method gave conservative predictions for G3 midspan moments and nonconservative predictions of G1 midspan moments, whereas the finite-element model gave conservative predictions of both G3 and G1 moments.

Computer simulations also were used to assess the sensitivity of equilibrium evaluations of the construction tests to changes in instrument readings. Monte Carlo simulations, run using commercially available software, were used to study the cumulative influence of instrument resolution variability on equilibrium results. These studies indicated that both force and moment equilibria were sensitive to small cumulative changes in readings supplied by resistance strain gauges affixed to cross-frame members ($\pm 5\mu\varepsilon$). These cumulative changes could result from using data acquisition systems with varying resolution levels to acquire data or from unwanted electrical noise being introduced into these systems during testing.

ACKNOWLEDGMENTS

This work was supported for the Georgia Institute of Technology by HDR Engineering through FHWA under Contract No. DTFH61-92-C-00136. Sheila Duwadi serves as the Contracting Officer's Technical Representative for FHWA. The assistance of Jim Burrell of Qualcomm, Inc., with preparation of this manuscript is greatly appreciated. In addition, the advice of Dr. Abdul-Hamid Zureick and Dr. Roberto Leon at the Georgia Institute of Technology has been invaluable for completing this research. The assistance of Bill Wright of FHWA, Joey Hartmann of Professional Service Industries, Inc., Dann Hall and Mike Grubb of BSDI, and John Yadlosky of HDR is appreciated.

REFERENCES

1. American Association of State Highway and Transportation Officials, *Guide Specifications for Horizontally Curved Bridges*, Washington, 1980, 1993.
2. American Institute of Steel Construction, *Highway Structures Design Handbook*, Vol. I, Chap. 12: V-Load Analysis, Chicago, IL, 1996.
3. Arizumi, Y., Hamada, S. & Oshiro, T., Static behavior of curved composite box girders, *Transactions of the Japanese Society of Civil Engineers*, **15** (1983), 212–6.
4. Brennan, P. J., Horizontally curved bridges first annual report: Analysis of horizontally curved bridges through three-dimensional mathematical model and small scale structural testing, Syracuse University, First Annual Report, Research Project HPR-2(111), November 1970.
5. Brennan, P. J., Horizontally curved bridges second annual report: Analysis of Seekonk River Bridge small scale structure through three-dimensional mathematical model and small scale structural testing, Syracuse University, Second Annual Report, Research Project HPR-2(111), November 1971.
6. Brennan, P. J., Analysis and structural testing of a multiple configuration small scale horizontally curved highway bridge, Syracuse University, Research Project HPR-2(111), December 1974.
7. Brennan, P. J., Antoni, C. M., Leininger, R. & Mandel, J. A., Analysis for stress and deformation of a horizontally curved bridge through a geometric structural model, Syracuse University Department of Civil Eng., Special Research Report No. SR-3, August 1970.
8. Brennan, P. J. & Mandel, J. A., Multiple configuration curved bridge model studies, *ASCE Journal of the Structural Division*, **105** (ST5) (1979), 875–90.
9. Culver, C. G. & Christiano, P. P., Static model tests of curved girder bridge, *ASCE Journal of the Structural Division*, **95** (ST8) (1969), 1599–1614.
10. Fam, A. R. & Turkstra, C., Model study of horizontally curved box girder, *ASCE Journal of the Structural Division*, **102** (ST5) (1976), 1097–1108.
11. Fiechtl, A. L., Fenves, G. L. & Frank, K. H., Approximate analysis of horizontally curved girder bridges, Texas University, Austin, Center for Transportation Research, Final Report No. FHWA-TX-91-360-2F, November 1987.
12. Fukumoto, Y. & Nishida, S., Ultimate load behavior of curved I-beams, *ASCE Journal of the Engineering Mechanics Division*, **107** (EM2) (1981), 367–84.
13. Galambos, T. V., Hajjar, J. F., Leon, R. T., Huang, W., Pulver, B. E. & Rudie, B. J., Stresses in steel curved girder bridges, Minnesota Department of Transportation Report No. MN/RC-96/28, August 1996.
14. Hajjar, J. F. & Boyer, T. A., Live load stresses in steel curved girder bridges, Progress Report on Task 1 for Minnesota Department of Transportation Project 74708, December 1997.
15. Hanshin Expressway Public Corporation, Guidelines for the design of horizontally curved girder bridges (draft), 1988.
16. Hibbitt, Karlsson & Sorenson, Inc., *Introduction to ABAQUS/Pre*, Version 5.8, Pawtucket, RI, 1998.
17. Hibbitt, Karlsson & Sorenson, Inc., *ABAQUS/Post Manual*, Version 5.8, Pawtucket, RI, 1998.

18. Hibbitt, Karlsson & Sorenson, Inc., *ABAQUS/Standard User's Manual*, Version 5.8, (1–3), Pawtucket, RI, 1998.
19. Linzell, D. G., Studies of a full-scale horizontally curved steel I-girder bridge system under self-weight, Ph.D. dissertation, School of Civil and Environmental Engineering, Georgia Institute of Technology, 1999.
20. MacNeal-Schwendler Corporation, *MSC/PATRAN Users Manual*, Los Angeles, CA, 1998.
21. Mozer, J., Cook, J. & Culver, C., Horizontally curved highway bridges: Stability of curved plate girders, Carnegie Mellon University Report No. P3, Research Project HPR-2(111), January 1973.
22. Pulver, B. E., Measured stresses in a steel curved bridge system, M.C.E. Report, Department of Civil Engineering, University of Minnesota, 1996.
23. Sennah, K. & Kennedy, J. B., Shear distribution in simply-supported curved composite cellular bridges, *ASCE Journal of Bridge Engineering*, **3** (2) (19xx), 47–55.
24. Shanmugam, N. E., Thevendran, J. Y., Liew, R., Tan, L. O., Experimental study on steel beams curved in plan, *ASCE Journal of Structural Engineering*, **121** (2) (1995), 249–59.
25. Thevendran, J. Y., Shanmugam, N. E. & Liew, R., Flexural torsional behavior of steel I-beams curved in plan, *Journal of Constructional Steel Research*, **46** (1–3), (1998), 79–80.
26. Vanguard Software Corporation, *DecisionPro for Windows*, version 3.0.4, demonstration version, Cary, NC, 1998.
27. Yoo, C. H. & Carbine, R. L., Experimental and analytical study of horizontally curved steel wide flanged beams, in *Proceedings, Structural Stability Research Council Annual Technical Session: Stability of Plate Structures*, Washington, 1985, pp. 131–43.
28. Zureick, A., Linzell, D., Leon, R. T. & Burrell, J., Curved steel I-girder bridges: Experimental and analytical studies, *Engineering Structures*, **22** (2) (2000), 180–90.
29. Zureick, A. & Naqib, R., Horizontally curved steel I-girder state-of-the-art analysis methods, *ASCE Journal of Bridge Engineering*, **4** (1), (1999), 38–47.
30. Zureick, A., Naqib, R. & Yadlosky, J. M., Curved steel bridge research project, interim report I: Synthesis, HDR Engineering, Inc., Publication No. FHWA-RD-93-129, December 1994.